

THE INFLUENCE OF FIBER ORIENTATION ON THE MECHANICAL FLOW PROPERTIES OF A CHOPPED FIBER REINFORCED THERMOPLASTIC COMPOSITE

P. THEVENIN and D. PERREUX
Laboratoire de Mécanique Appliquée R. Chaléat
Faculté des Sciences et des Techniques
Route de Gray
25030 Besançon CEDEX - France

Abstract. In this paper, the change of fiber orientation that occurs during the molding flow of a composite material, based on a thermoplastic matrix reinforced by chopped fibers, is investigated. The fiber orientation is described by a distribution function which is divided in two elementary distribution functions, each of which is concerned with part of the fibers. The model presents the changes of these functions, taking into account the interaction between all fibers and the transversal shear. The model agrees with experimental data obtained in the flow of composites in plate type geometry.

INTRODUCTION

Short fiber reinforced thermoplastics are usually processed by injection or compression molding. The properties of such materials depend to a great extent on fiber content, fiber length and fiber orientation. While the first two parameters are mainly determined by the composition of the material, the latter is a function of the local flow in the mold cavity. Fiber orientation, besides reinforcing the material, causes considerable anisotropy with regard to a number of mechanical properties.

Some authors have already developed models to predict flow properties, such as flow stress, for highly anisotropic fluids [1,2,3], fluid streamlines [4] and to reach orientation distribution in complex geometries [5,6].

In this study, we have developed a model to predict fiber orientation before being included in a previous model of anisotropic viscosity [7] in order to couple flow fluid with fiber orientation changes through the flow molding process.

EXPERIMENTAL METHOD

The composite preforms (polypropylene, 30% fiber-glass) with unidirectional fiber orientation (photo 1) are placed in a mold heated to 200°C (Fig. 1). This

temperature is above the melting point but slightly below the degradation temperature. During the flow, the temperature is constant at the mold surface, but a temperature gradient is observed between this surface and the center of the sample which makes it necessary to take into account the thermal exchange in the flow. After compression, the plates are quickly cooled, with constant pressure, in order to reduce the porosity [8,9].

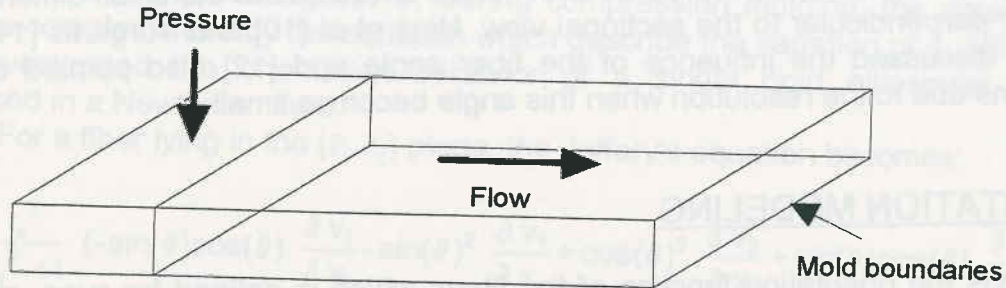


Fig. 1 - Molding flow geometry with a transversal composite preform

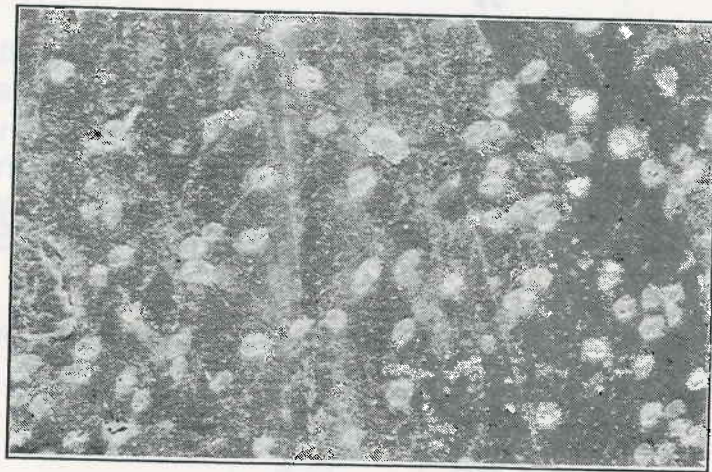


Photo 1 - Micrography of a preform having unidirectional fiber orientation

The samples are cut from the center part of these plates, which makes it possible to disregard the "end effect". Samples are taken at several points along the axial direction (Fig. 2), in order to analyze the change of the fiber orientation with the flow.

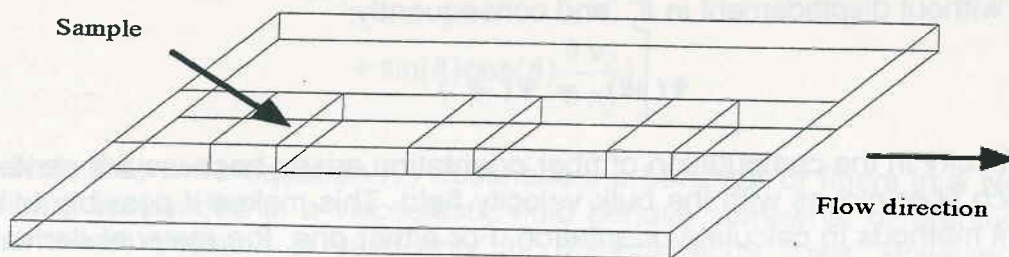


Fig. 2 - Position of the samples used in micrographical experiments

For each sample, the faces perpendicular to the flow are prepared for SEM observation.

Measurement of fiber orientation in the sample is based on an analysis of the ratio between the length of the axes of the ellipse produced by the sectional view of the fibers. Each sample supplies about one thousand units of data, which makes it possible to obtain a statistic distribution of the orientation at several points of the plate.

Great care must be taken during this measurement stage. In particular, the angle of the cut must be considered to minimize errors due to the small dimension of the fiber perpendicular to the sectional view. Hine et al [10] and Yurgartis [11] have already discussed the influence of the fiber angle and [12] also pointed out the limitations due to the resolution when this angle becomes small.

ORIENTATION MODELING

Ψ is the orientation function of the fibers which is defined for every material point of the flow. Ψ must verify the normalization and the condition of symmetry:

$$\int_0^{2\pi} \Psi(\theta) d\theta = 1 \quad (1)$$

$$\Psi(\theta) = \Psi(\theta + \pi) \quad (2)$$

Taking into account a planar orientation of the fiber, only θ is useful to provide the orientation of the fibers (Fig. 3).

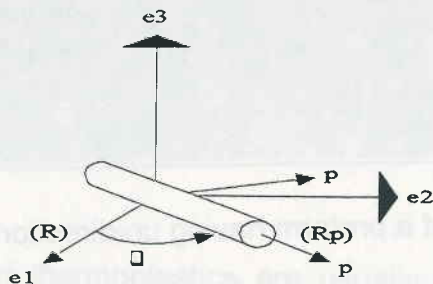


Fig. 3 - Orthonormal reference axis describing fiber orientation

The vector \bar{p} lies in the same direction as the fibers. The flow is in the direction \bar{e}_1 without displacement in \bar{e}_2 and consequently:

$$\Psi(+\theta) = \Psi(-\theta) \quad (3)$$

A difficulty in the computation of fiber orientation arises because the center of mass of each fiber moves with the bulk velocity field. This makes it possible to use two different methods to calculate orientation. For either one, the material derivative can be used to formulate an equation for the orientation at fixed points. Or, the trajectories of individual fluid particles can be followed, integrating the fiber orientation equations for the velocity gradients experienced by the particle.

In this study, to supply the change of the distribution the method which consists in using material derivative is adopted in fixed points of a meshed surface tied up to the material field at each point in time. The fiber density is assumed to be

constant at each point of the plate. The conservation condition must be verified, by the function Ψ :

$$\frac{D\Psi}{Dt} = -\frac{\partial(\Psi\dot{\theta})}{\partial\theta} \quad (4)$$

To provide the change in Ψ , during compression molding, the equation (4) must be complemented by the equation which describe the variation of θ . Jeffery [13] first investigated the orientation behavior of a single rigid ellipsoidal particle immersed in a Newtonian fluid.

For a fiber lying in the (\bar{e}_1, \bar{e}_2) plane, the Jeffery's equation becomes:

$$\dot{\theta} = \frac{r_e^2}{r_e^2 + 1} (-\sin(\theta)\cos(\theta)) \frac{\partial v_1}{\partial x_1} - \sin(\theta)^2 \frac{\partial v_1}{\partial x_2} + \cos(\theta)^2 \frac{\partial v_2}{\partial x_1} + \sin(\theta)\cos(\theta) \frac{\partial v_2}{\partial x_2} - \frac{1}{r_e^2 + 1} (-\sin(\theta)\cos(\theta)) \frac{\partial v_1}{\partial x_1} + \cos(\theta)^2 \frac{\partial v_1}{\partial x_2} - \sin(\theta)^2 \frac{\partial v_2}{\partial x_1} + \sin(\theta)\cos(\theta) \frac{\partial v_2}{\partial x_2} \quad (5)$$

The quantity r_e is called the equivalent ellipsoidal axis ratio. For a cylindrical fiber with a large aspect ratio, r_e becomes infinite. This model can be applied to a low-concentration suspension of fibers in which one fiber is supposed to be free from each of the others.

For a concentrated suspension, Folgar and Tucker [14] have proposed that the angular velocity of the fibers can be approximated by:

$$\dot{\theta} = -\sin(\theta)\cos(\theta) \frac{\partial v_1}{\partial x_1} - \sin(\theta)^2 \frac{\partial v_1}{\partial x_2} + \cos(\theta)^2 \frac{\partial v_2}{\partial x_1} + \sin(\theta)\cos(\theta) \frac{\partial v_2}{\partial x_2} - \frac{C_1 \dot{\gamma}}{\Psi} \frac{\partial \Psi}{\partial \theta} \quad (6)$$

The extra term is used to describe the interaction between the fibers. C_1 is a parameter, $\dot{\gamma}$ is the scalar magnitude of the strain rate tensor. Combining equations (4) and (6) gives:

$$\frac{D\Psi}{Dt} = C_1 \dot{\gamma} \frac{\partial^2 \Psi}{\partial \theta^2} - \frac{\partial}{\partial \theta} \left[\Psi \left(-\sin(\theta)\cos(\theta) \frac{\partial v_1}{\partial x_1} - \sin(\theta)^2 \frac{\partial v_1}{\partial x_2} + \cos(\theta)^2 \frac{\partial v_2}{\partial x_1} + \sin(\theta)\cos(\theta) \frac{\partial v_2}{\partial x_2} \right) \right] \quad (7)$$

Note that while equation (7) describes the behavior of fibers in a Newtonian fluid, fibers suspended in a viscoelastic fluid behave somewhat differently. What's more, the last equation is valid only for homogeneous flows. However, it is a reasonable approximation when the length scale over which velocity gradients change is large compared to the fiber length.

For all distribution around a material point, the strain rate is assumed to be constant.

Using the tensorial notation introduced by Advani and Tucker [15] equation (7) can be written:

$$\frac{da_{ij}}{dt} = -\frac{1}{2} (\omega_{ik} a_{kj} - a_{ik} \omega_{kj}) + \frac{1}{2} (\dot{\gamma}_{ik} a_{kj} + a_{ik} \dot{\gamma}_{kj}) - a_{ijkl} \dot{\gamma}_{kl} + 2 C_1 \dot{\gamma} (\delta_{ij} - 2 a_{ij}) \quad (8)$$

with:

$$\dot{\gamma}_{ij} = \frac{\partial v_j}{\partial x_i} + \frac{\partial v_i}{\partial x_j} \quad \text{and} \quad \omega_{ij} = \frac{\partial v_j}{\partial x_i} - \frac{\partial v_i}{\partial x_j}$$

$$[a_2] = a_{ij} = \int_0^{2\pi} p_i p_j \Psi(\theta) d\theta$$

$$[a_4] = a_{ijkl} = \int_0^{2\pi} p_i p_j p_k p_l \Psi(\theta) d\theta$$

Indeed, it is easier to express an average value of a_{ijkl} noted $\overline{a_{ijkl}}$ such as:

$$\overline{a_{ijkl}} = (1-f) \hat{a}_{ijkl} + f \tilde{a}_{ijkl} \quad (9)$$

where \hat{a}_{ijkl} is a linear closure approximation exact for a completely random distribution which has the form:

$$\hat{a}_{ijkl} = -\frac{1}{24} (\delta_{ij} \delta_{kl} + \delta_{ik} \delta_{jl} + \delta_{il} \delta_{jk}) + \frac{1}{6} (a_{ij} \delta_{kl} + a_{ik} \delta_{jl} + a_{il} \delta_{jk} + a_{kl} \delta_{ij} + a_{jl} \delta_{ik} + a_{jk} \delta_{il})$$

and \tilde{a}_{ijkl} is a quadratic closure already used by Lipscomb [15]:

$$\tilde{a}_{ijkl} = a_{ij} a_{kl}$$

f is a generalization of Herman's orientation factor expressed as:

$$f = 2 a_{ij} a_{ji} - 1$$

This scalar measure of orientation is more accurate to build up the hybrid approximation $\overline{a_{ijkl}}$.

We next consider an initial distribution Ψ with a perfect uniaxial alignment of the fibers in the \vec{e}_2 direction. The integration result of equation (8) for a such distribution gives a symmetrical distribution with only one maximum either over \vec{e}_2 or \vec{e}_1 for sufficient time. However an analysis of the experimental results shows that the resulting distribution has two maximums for each point of the flow (Fig. 4).

Fig. 4

To
of two ter

$\Psi^+ =$

$\Psi^- =$

In tensoria

where:

with:

Next
is obtained

TRANSVI

Expe
regard as t
with a Hele-
orientation
orientation
the Ψ max
orientation a
the following
sum of sever

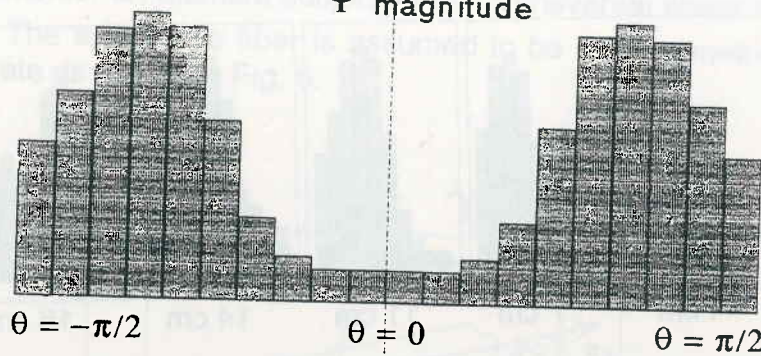
Ψ magnitude

Fig. 4 - Cleavage of the initial distribution in two elementary statistic function

To take this result into account, the Ψ distribution is supposed to be the sum of two terms Ψ^+ and Ψ^- given as:

$$\Psi^+ = 2\Psi \text{ when } \theta \in [0, \pi/2] \cup [\pi, 3\pi/2] \text{ and } 0 \text{ when } \theta \in [\pi/2, \pi] \cup [3\pi/2, 2\pi]$$

$$\Psi^- = 2\Psi \text{ when } \theta \in [\pi/2, \pi] \cup [3\pi/2, 2\pi] \text{ and } 0 \text{ when } \theta \in [0, \pi/2] \cup [\pi, 3\pi/2]$$

In tensorial expression it becomes:

$$[a_2] = \frac{1}{2} ([a_2^+] + [a_2^-])$$

where:

$$[a_2^+] = \begin{bmatrix} a_{11} & a_{12} \\ a_{21} & a_{22} \end{bmatrix} \text{ and } [a_2^-] = \begin{bmatrix} a_{11} & -a_{12} \\ -a_{21} & a_{22} \end{bmatrix}$$

with:

$$a_{21} = a_{12}$$

Next, the equation of change will be applied only to the Ψ^+ distribution and Ψ^- is obtained from the various symmetrical considerations.

TRANSVERSAL SHEAR CONTRIBUTION

Experimental results reveal a motion of both maximum of the Ψ distribution as regard as the position in the flow. However the use of the equation of change (8) with a Hele-Shaw model for the flow field is not accurate for describing this particular orientation considering either a bidimensional or a tridimensional expression of the orientation tensors. The next figure (Fig. 5) makes it possible to track the motion of the Ψ maximum defined for $\theta \in [0, \pi/2]$. Two photos also give a view of the orientation at the constituents scale for two different positions in the molding plate. In the following, it will be considered that the full angular velocity $\dot{\theta}$ can be written as a sum of several terms corresponding to the various phenomena investigated as:

$$\dot{\theta} = \sum_i \dot{\theta}_i \text{ where } \dot{\theta}_1 \text{ represents the Jeffery's equation}$$

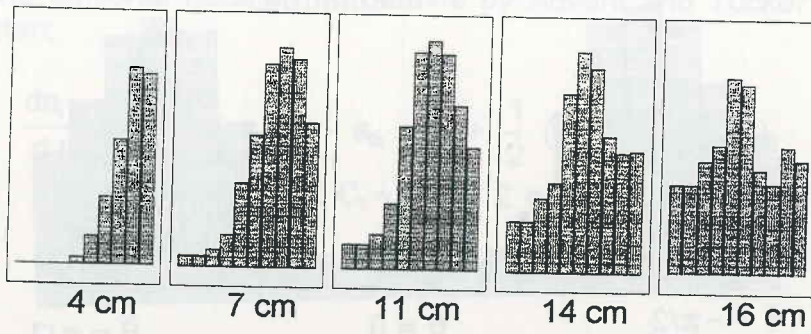


Fig. 5 - Evolution of the experimental statistic distribution through the molding plate

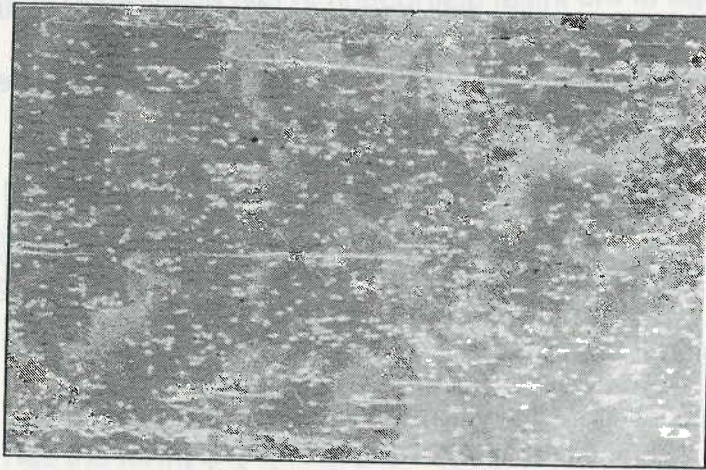


Photo 2 - Micrography of a sample cut at 4 cm from the beginning of the mold

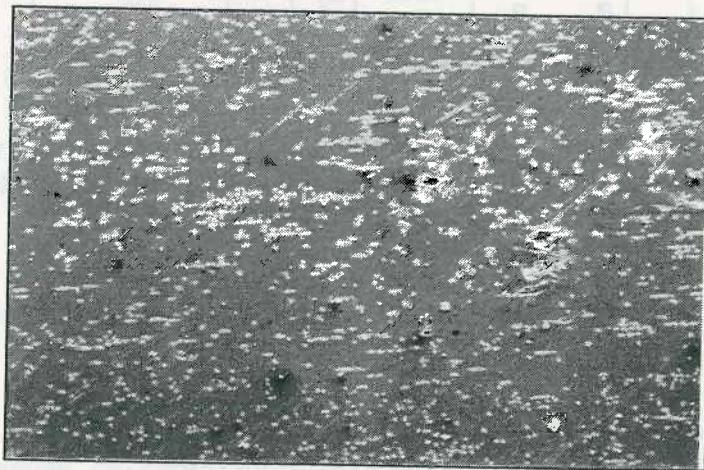


Photo 3 - Micrography of a sample cut at 14 cm from the beginning of the mold

According to the initial distribution state and the mold-filling flow, the motion of the fibers is supposed to be planar at every point in time. Fiber orientation is then expressed in each finite element using a planar state and each element is supposed to interact with the others through the transversal shear induced by the flow velocity field.

Le
only one
relative s

The
rate on its
motion ex

This term :

INTERAC

For
orientation
effect of in
in equation
another mo
motion is p

Let us consider an element subjected to a transversal shear rate $\dot{\gamma}_{13}$ including only one fiber. The axis of the fiber is assumed to be the symmetrical center of the relative shear rate as shown in Fig. 6.

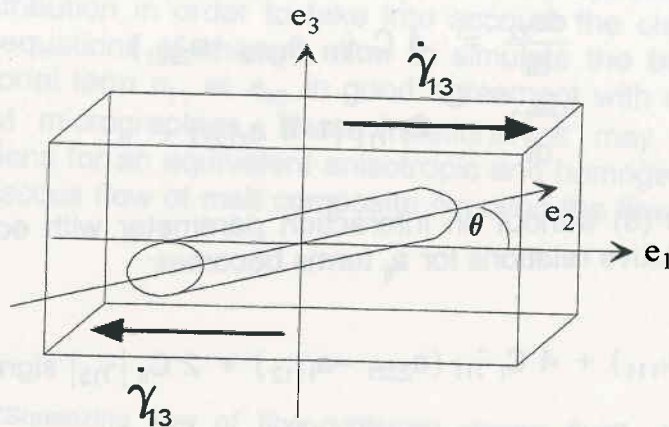


Fig. 6 - Fiber orientation is influenced by shear rate $\dot{\gamma}_{13}$

Then, the fiber is considered to be under a fluid drive motion due to the shear rate on its diameter. The resulting motion has the form of an incremental rotational motion expressed as:

$$\dot{\theta}_2 = -C_{II} \cos(\theta) \sin(\theta) |\dot{\gamma}_{13}| \text{sign}(\dot{\gamma}_{11}) \quad (10)$$

This term adds the following tensorial terms to equation (8):

$$\begin{aligned} \frac{da_{11}}{dt} &= 2 C_{II} |\dot{\gamma}_{13}| \text{sign}(\dot{\gamma}_{11}) (a_{11} - a_{1111}) \\ \frac{da_{22}}{dt} &= -2 C_{II} |\dot{\gamma}_{13}| \text{sign}(\dot{\gamma}_{11}) a_{2211} \\ \frac{da_{12}}{dt} &= C_{II} |\dot{\gamma}_{13}| \text{sign}(\dot{\gamma}_{11}) (a_{2221} - a_{1112}) \end{aligned} \quad (11)$$

INTERACTION BETWEEN FIBERS

For the particular flow considered here and especially regarding the initial orientation distribution, the phenomenological coefficient modeling the randomizing effect of interactions between particles introduced previously by Folgar and Tucker in equation (6) seems not to be accurate to describe the behavior of the a_{12} term. So another model using the active part of the strain rate tensor on the rotational fiber motion is proposed:

$$\begin{aligned} \dot{\theta}_3 = -\frac{C_I}{\Psi} \frac{\partial \Psi}{\partial \theta} & \left(-\sin(\theta) \cos(\theta) \frac{\partial v_1}{\partial x_1} - \sin(\theta)^2 \frac{\partial v_1}{\partial x_2} \right. \\ & \left. + \cos(\theta)^2 \frac{\partial v_2}{\partial x_1} + \sin(\theta) \cos(\theta) \frac{\partial v_2}{\partial x_2} \right) \end{aligned} \quad (12)$$

With the flow field chosen, one gets using tensorial notation:

$$\begin{aligned}\frac{da_{11}}{dt} &= 4 C_1 \dot{\gamma}_{11} (a_{2221} - a_{1112}) \\ \frac{da_{22}}{dt} &= 4 C_1 \dot{\gamma}_{11} (a_{1112} - a_{2221}) \\ \frac{da_{12}}{dt} &= C_1 \dot{\gamma}_{11} (1 - 8 a_{1122})\end{aligned}\quad (13)$$

Combining equation (8) without an interaction parameter with equations (11) and (13), the final constitutive relations for a_{ij} terms becomes:

$$\frac{da_{11}}{dt} = \dot{\gamma}_{11} (a_{11} - a_{1111}) + 4 C_1 \dot{\gamma}_{11} (a_{2221} - a_{1112}) + 2 C_{II} |\dot{\gamma}_{13}| \text{sign}(\dot{\gamma}_{11}) (a_{11} - a_{1111})$$

$$\frac{da_{22}}{dt} = -\dot{\gamma}_{11} a_{2211} + 4 C_1 \dot{\gamma}_{11} (a_{1112} - a_{2221}) - C_{II} |\dot{\gamma}_{13}| \text{sign}(\dot{\gamma}_{11}) a_{2211}$$

$$\frac{da_{12}}{dt} = \dot{\gamma}_{11} \left(\frac{a_{12}}{2} - a_{1122} \right) + C_1 \dot{\gamma}_{11} (1 - 8 a_{1122}) + C_{II} |\dot{\gamma}_{13}| \text{sign}(\dot{\gamma}_{11}) (a_{2221} - a_{1112})$$

RESULTS AND DISCUSSION

The molding tests were performed with a constant compression velocity of 5 mm/s. A numerical solution was obtained for each element of a meshed surface from the previous equations of change. Then the a_{ij} terms obtained by an average value for a given position were compared (Fig. 7) with simulate results for various points in the final plate.

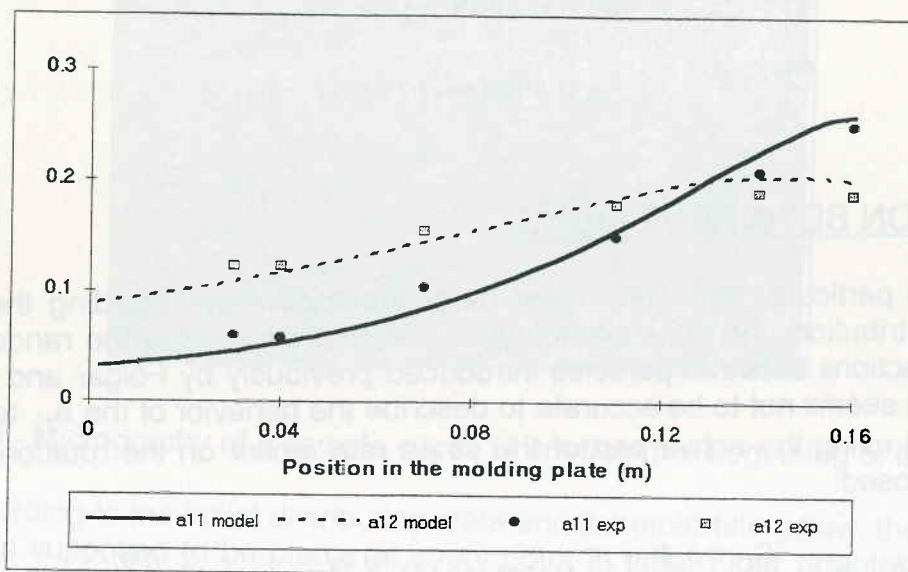


Fig. 7 - Correlation of experimental results and simulation

CONCL

TH
distributi
two stati
distributi
independ
issued fr
constitut
descripti
fiber orie

REFERE

- [1] - T.G. Mathematic
- [2] - M.R. compound i
- [3] - L. Czar characteristi
- [4] - G.G. Li of Non-Newt
- [5] - V. Verle parts",
- [6] - G. Ausi reinforced th
- [7] - P. The thermoplastic
- [8] - R.J. Wa mixing", Jour
- [9] - Y. Leter
- [10] - P.J. Hi
- [11] - S.W. fiber reinforc
- [12] - P.A. O' Technology,
- [13] - G.B. Jef
- [14] - F.P. Fe
- [15] - S.G. Ad
- [16] - G.G. Lip

CONCLUSION

The behaviour of an anisotropic melt composite with any orientation distribution has been investigated. The model which is proposed requires the use of two statistical distribution in order to take into account the cleavage of the initial distribution. The equations of change allow to simulate the behaviour of the two independent tensorial term a_{11} et a_{12} in good agreement with experimental results issued from SEM micrographies. These relationships may be used with the constitutive equations for an equivalent anisotropic and homogeneous fluid to get a description of a viscous flow of melt composite coupling the flow properties with the fiber orientation.

REFERENCES

- [1] - T.G. Rogers, "Squeezing flow of fiber-reinforced viscous fluid", *Journal of Engineering Mathematics*, 23, (1989), 81-89.
- [2] - M.R. Barone and D.A. Caulk, "A model for the flow of a chopped fiber reinforced polymer compound in compression molding", *Journal of Applied Mechanics*, 53, (1986), 361-371.
- [3] - L. Czamecki and J.L. White, "Shear flow rheological properties, fiber damage, and mastication characteristics of aramid, glass, and cellulose fiber reinforced polystyrene melts", *Journal of Applied Polymer Science*, 25, (1980), 1217-1244.
- [4] - G.G. Lipscomb and M.M. Denn, "The flow of fiber suspensions in complex geometries", *Journal of Non-Newtonian Fluid Mechanics*, 26 (1988), 297-325.
- [5] - V. Verleye, A. Courniot and F. Dupret, "Prediction of fiber orientation in complex injection molded parts",
- [6] - G. Ausias, M. Vincent, J.F. Agassant, J. Jarrin and F. Dawans, "Extrusion of short glass fiber reinforced thermoplastic in pipe die",
- [7] - P. Thevenin, D. Perreux and D. Varchon, "Flow simulation of chopped fibers reinforced thermoplastic composite in plate type geometry", in *Proceeding of Advancing with Composites '94*, Milan, May 1994.
- [8] - R.J. Watson and C.E. Chaffey, "Void content of a viscoelastic composite melt: reduction during mixing", *Journal of Polymer Composites*, 7(6), (1986), 442-447.
- [9] - Y. Leterrier, "Evolution rhéologique et structurale d'un composite polypropylène/fibers de verre lors de son estampage", Ph.D Thesis, Institut National Polytechnique de Lorraine, Nancy, (1991).
- [10] - P.J. Hine, R.A. Duckett, N. Davidson and A.R. Clarke, "Modeling of the elastic properties of fiber reinforced composites. I: orientation measurement", *Journal of Composites Science and Technology*, 47, (1993), 65-73.
- [11] - S.W. Yurgartis, "Measurement of small angle fiber misalignments in continuous fiber composites", *Journal of Composites Science and Technology*, 30, (1987), 279-293.
- [12] - P.A. O'Connell and R.A. Duckett, "Measurements of fiber orientation in short-fiber reinforced thermoplastics", *Journal of Composites Science and Technology*, 42, (1991), 329-347.
- [13] - G.B. Jeffery, "The motion of ellipsoidal particles immersed in a viscous fluid", *Proc. Roy. Soc.*, A102, (1922), 161-179.
- [14] - F.P. Folgar and C.L. Tucker, "Orientation behavior of fibers in concentrated suspensions", *Journal of Reinforced Plastic Composites*, 3(4), (1984), 98-119.
- [15] - S.G. Advani and C.L. Tucker, "The use of tensors to describe and predict fiber orientation in short fiber composites", *Journal of Rheology*, 31(8), (1987), 751-784.
- [16] - G.G. Lipscomb, "Analysis of suspension rheology in complex flows", Ph.D. Thesis, University of California, Berkeley, (1986).